*Int. J. Electrochem. Sci.*, 13 **(2018)** 1614 – 1628, doi: 10.20964/2018.02.56

**International Journal of ELECTROCHEMICAL SCIENCE**
www.electrochemsci.org

# Effect of the Degree of Rolling Reduction on the Stress Corrosion Cracking Behavior of SUS 304 Stainless Steel

*Shanlin He*[*], *Daming Jiang*

School of Materials Science and Engineering, Harbin Institute of Technology, Harbin 150001, China
[*]E-mail: 11b909025@hit.edu.cn

*Received:* 23 October 2017 / *Accepted:* 14 December 2017 / *Published:* 28 December 2017

In this study, SUS 304 stainless steel was cold rolled with various degrees of rolling reduction. The microstructure and stress corrosion cracking behavior before and after cold rolling were investigated. Electrochemical noise measurements coupled with slow strain rate testing were performed in a 3.5% NaCl solution. The results indicated that the microstructure of SUS 304 stainless steel transformed from a single austenite phase into a compound with both the martensite phase and original austenite phase after cold rolling. The martensite phase increased with an increase in the degree of rolling reduction. During the slow strain rate test process, mechanical properties such as the breaking elongation and tension strength, corrosion resistance and stress corrosion cracking resistance significantly decreased after cold rolling. All the rolled specimens, the mechanical properties were highest for the specimen when the degree of rolling reduction was 14%. The stress corrosion cracking susceptibility depended on the crack initiation time during the slow strain rate test process.

**Keywords:** SUS 304 stainless steel; cold rolling; stress corrosion cracking; electrochemical noise; slow strain rate test

## 1. INTRODUCTION

Steel has been one of the most important structural materials due to its excellent mechanical properties and corrosion resistance[1-13]. Under corrosive environments and applied loads, stress corrosion cracking is a performance deterioration process and a serious problem for steel, especially stainless steel, which has been widely investigated all over the world[14-20]. For instance, Johns investigated 304 stainless steel nuts with an applied torque of approximately 80% of the yield strength value, and when immersed in a 3% NaCl solution at 35 ℃, transgranular stress corrosion cracking occurred in one nut after 12 months and in the other two nuts after 21 months[21]. Okada reported that the fracture mode of solid solution-treated 304 stainless steel was transgranular in a 42% MgCl2

solution at a temperature of 143 ℃, and almost intergranular when the solution concentration was 25% at a temperature of 115 ℃[22]. Szklarska-Snialowska summarized the minimum oxygen content for stress corrosion cracking of sensitized 304 stainless steel in high-temperature water at different temperatures using slow strain rate testing[23]. Singh indicated that the fracture mode of cold-rolled and sensitized 304 stainless steel in polythionic acid showed dimples when the degree of rolling reduction values were 60% and 80%, and when the degree of rolling reduction values were 20% and 40%, the fracture mode was intergranular[24]. Cragnolino found that intergranular stress corrosion cracking occurred for sensitized 304 stainless steel in a $H_2SO_4$ solution at a concentration of more than 3%; however, cracking did not occur at a concentration less than 3% after 60 days[25]. Li observed the intergranular stress corrosion cracking behavior for type I and type III WOL specimens of sensitized 304 stainless steel in a $Na_2S_2O_3$ solution at a concentration of $7\times10^{-4}$ mol/L and a temperature of 50 ℃, and found that the $K_{ISCC}$ was 20 MPa/$m^{1/2}$ and the *da*/*dt* values for type I and type III WOL specimens were $4\times10^{-6}$/s and $4\times10^{-6}$/s, respectively[26].

With the development and application of 304 stainless steel, cold rolling has been extensively used and is considered to be beneficial to the mechanical properties of steel due to work hardening but harmful to the corrosion resistance due to the martensite phase formed during the rolling process[27-29]. Nevertheless, according to the author's knowledge, the effect of cold rolling on the stress corrosion cracking behavior of 304 stainless steel has not been fully elucidated, so the related research has great practical significance. Therefore, we focued on the influence of cold rolling, and the results in the present study could be very useful for studying stress corrosion cracking prevention technology of the cold worked 304 stainless steel.

## 2. EXPERIMENTAL

### *2.1 Materials*

A commercially available SUS 304 stainless steel sheet at a thickness of 3 mm was used in this work. The chemical composition is shown in Table 1.

**Table 1.** Chemical compositions (wt.%) of SUS 304 stainless steel sheets.

| Element | Fe | C | Si | Cr | Mn | Ni | P | S |
|---|---|---|---|---|---|---|---|---|
| Content | Balance | ≤0.08 | ≤1.00 | 18.00~20.00 | ≤2.00 | 8.00~11.00 | ≤0.045 | ≤0.03 |

### *2.2. Heat treatment and cold rolling*

To obtain a single austenite phase and chemical homogeneity, a solution treatment was applied to the SUS 304 stainless steel sheets using the following process: the as-received sheets were heated to 1050 ℃, maintained for 30 min, and then quenched in water.

After solution treatment, the stainless steel sheets were cold rolled to various degrees of rolling reduction (8%, 14% and 23%) through plastic deformation by unidirectional rolling in a laboratory rolling mill. The content of the martensite phase induced by cold rolling in the specimen was determined by a ferrite content detector.

### *2.3. Slow strain rate test*

The stress corrosion cracking behavior of SUS 304 stainless steel was measured by LETRY WDL-1000 slow strain rate tester at a strain rate of $10^{-6}$/s in a 3.5% NaCl solution at room temperature. The dimensions of the tension specimen are shown in Figure 1.The tension specimens were covered with silicone rubber, and only the middle section with an area of 1 $cm^2$ was exposed to the test solution.

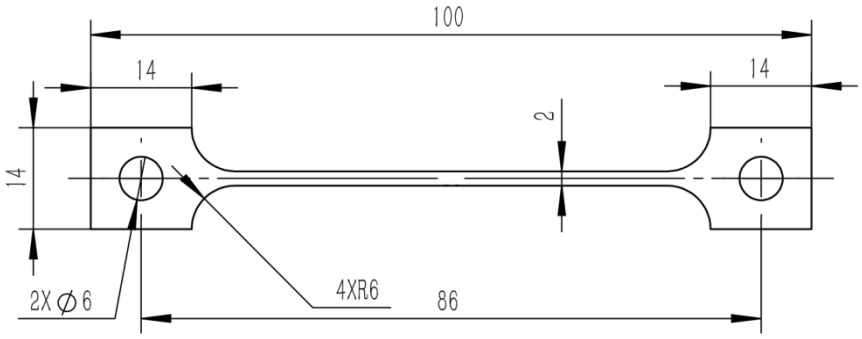


**Figure 1.** Dimensions of the tension specimen, mm.

### *2.4. Electrochemical noise measurements*

The stress corrosion cracking behavior of SUS 304 stainless steel was investigated by employing electrochemical noise using a Gamry Reference 3000 electrochemical measurement system coupled with slow strain rate testing. The modified electrochemical noise technology called electrochemical emission spectroscopy (EES) was employed in this study. The reference electrode was a saturated calomel electrode (SCE); the working electrode was the tension specimen; and a platinum wire tip called the microcathode was used as the counter electrode[30-32]. Electrochemical noise measurements without a bias voltage or current were performed every 5 h during the entire slow strain rate test process; the sampling time was 512 s, and the sampling frequency was 2 Hz for the data collection. The electrochemical noise data were analyzed using ESA 410 Analysis software.

### *2.5. Microstructure and fracture surface analysis*

The specimens were treated according to the standard metallographic preparation (cut, ground, polish and etch), and the microstructures were analyzed by an Olympus PMG2 light microscope.

The fracture analyses of the tension specimens were performed by SEM (Hitachi S-3000N)

## 3. RESULTS AND DISCUSSION

### *3.1 Microstructures of SUS 304 stainless steel before and after cold rolling*

The microstructures of SUS 304 stainless steel before and after cold rolling are shown in Figure 2. As shown in Figure 2a, the solution-treated specimen before cold rolling was composed of a single austenite phase. After cold rolling, a martensite phase (dark area) was distributed in the original austenite phase (bright area) boundaries. This effect was induced by plastic deformation during the cold rolling process, as shown in Figure 2b, Figure 2c and Figure 2d. When the degrees of rolling reduction were 8%, 14% and 23%, the contents of the martensite phase were 6%, 12% and 20%, respectively, which obviously increases with an increasing degree of rolling reduction and implies a decreasing content of the original austenite phase. For stainless steel, the formation of cold rolling-induced martensite was uncovered by other similar studies[33,34]. Wasnik found the apparent subdivision of the grains during the cold rolling process and that the split grain boundaries existed as packs. In comparison with specimens with lower degrees of rolling reduction, the grain subdivision was more extensive in the specimen with a higher degree of rolling reduction, and the strain-induced martensite increased monotonically with an increase in the degree of rolling reduction[35]. Mubarok indicated that the deformation caused a morphological change. The rolled free specimen consisted of equiaxed austenite grains that were randomly oriented, and the austenite phase underwent a shape change from an equiaxed structure to a needle-like structure. The change became increasingly apparent with an increase in the degree of rolling reduction, and the XRD results confirmed the deformation, which was introduced to the specimen that was transformed from the austenite phase into the martensite phase during the cold rolling process. As the degree of rolling reduction applied to the specimen increased, the more austenite grains changed to martensite grains, which showed a dual-phase structure in the rolled specimens[36]. Palit Sagar found that a non-rolled specimen showed essentially a single austenite phase, and the grain boundaries were faintly visible. Additionally, most of the coarse grains exceeded 50 μm; the martensite phase was observed in the rolled specimens; and the volume percentage of the martensite phase increased with an increasing degree of rolling reduction. It was quite clear that the slip lines and the twins had a bearing on the nucleation and growth of the martensite phase, and the phase nucleated at the intersections of the shear bands[37]. Wang revealed that a uniform matrix grain size and typical equiaxed austenitic grains with annealing twins were observed in the rolled free specimen, and a certain amount of board strip martensite could also be found in the austenitic substrate. Additionally, the martensite phase may result from the fabrication and manufacturing processes, and the rolled specimens showed a homogeneous distribution of martensite with a few residual primary ferrite islets in the matrix. The deformation-induced martensite phase content in the austenitic matrix monotonously increased with an increase in cold deformation (degree of rolling reduction) at room temperature, and the austenitic phase grains were compressed and elongated in the rolling direction[38].

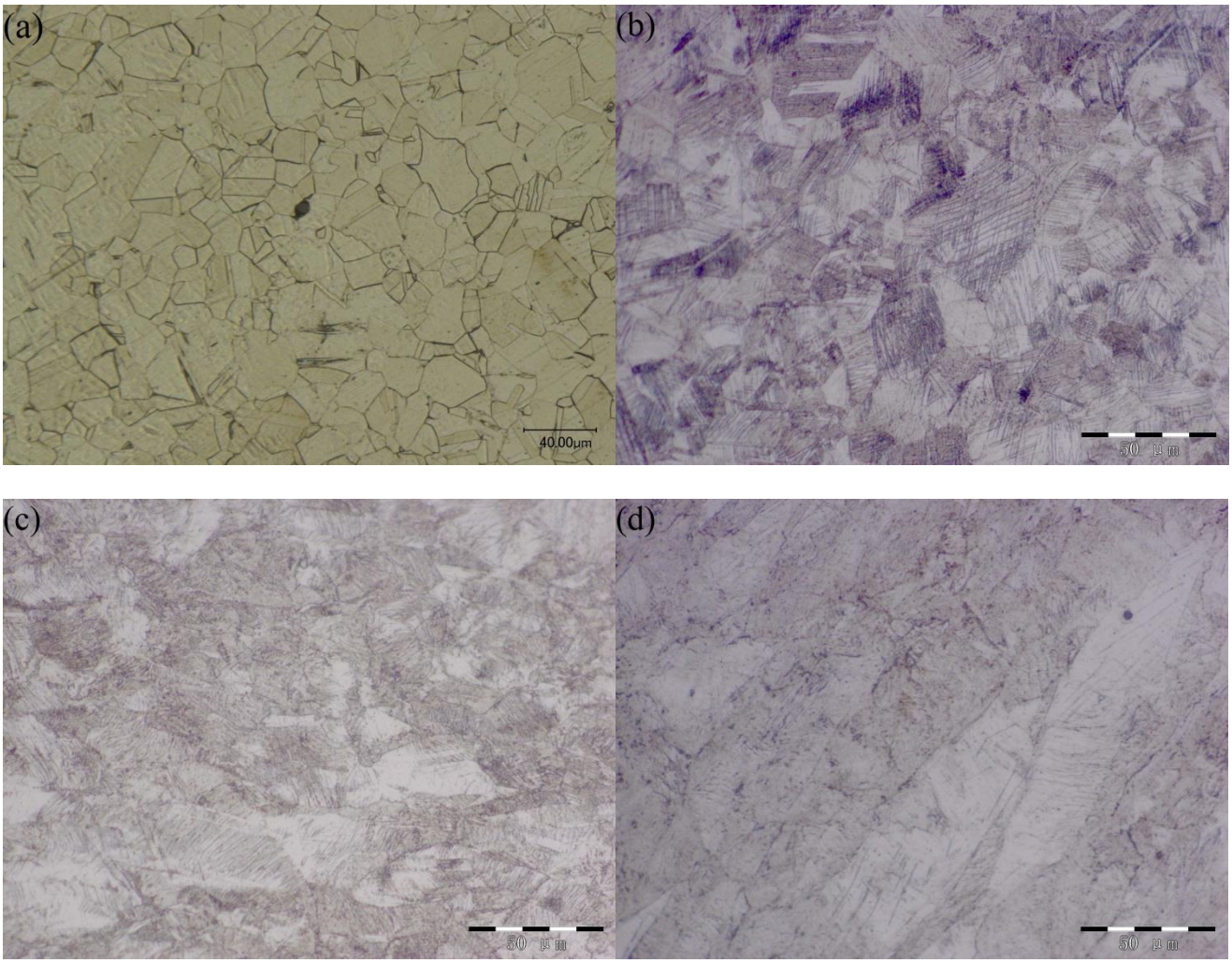


**Figure 2.** Microstructures of SUS 304 stainless steel before and after cold rolling: (a) specimen before cold rolling; (b) specimen when the degree of rolling reduction was 8%; (c) specimen when the degree of rolling reduction was 14%; and (d) specimen when the degree of rolling reduction was of 23%.

### *3.2. Slow strain rate test*

The slow strain rate test was employed to investigate the susceptibility of SUS 304 stainless steel to stress corrosion cracking. The stress-strain curves of the specimens before and after cold rolling during the slow strain rate test process are displayed in Figure 3. The results from stress-strain curves showed that the breaking elongation and tension strength of the specimen before cold rolling were 42% and 1123 MPa, respectively. There was an obvious degeneration in the mechanical properties of the specimens after cold rolling in comparison with the non-rolled specimen; the breaking elongation and tension strength of the specimen decreased by 81% and 42%, respectively, when the degree of rolling reduction was 23%. Note that the mechanical properties did not monotonously change with an increasing degree of rolling reduction. The specimen showed the highest breaking elongation and tension strength among all the rolled specimens when the degree of rolling reduction was 14%, which implied that this the specimen had the longest fracture time during the slow strain rate

test and lowest susceptibility to stress corrosion cracking. Figure 4 represents the fractograph morphologies of the specimens before and after cold rolling during the slow strain rate test process. There were no significant differences among the specimens, which all showed numerous dimples on the fracture surfaces and indicated that the fracture mode of all the specimens was dominated by ductile fractures. Compare with the rolled specimens, the fractograph of the non-rolled specimen displayed the biggest and deepest dimples on the fracture surface, which revealed the best plastic deformation capacity (plasticity) for the non-rolled specimen and was consistent with the conclusion obtained from the stress-strain curves in Figure 3. Similar studies were published by other authors[39-41]. Muraleedharan investigated the influence of cold work (degree in the range from 2.3% to 56%) on the stress corrosion cracking properties of AISI type stainless steel in a boiling $MgCl_2$ solution at 154 ℃. The results showed that at an applied stress of 112 MPa, the total time to fracture decreased with an increasing cold work level, reached a minimum value when the degree of cold work was 15% and then increased at higher cold work levels. Moreover, the total time to fraction decreased with an increase in the cold work level up to a certain degree (26%), and there was no significant change thereafter when the applied stress was 40% of the yield strength of the specimen. The stress corrosion cracking that was initiated from the transgranular mode transitioned to the intergranular mode as the crack proceeded and finally fractured in ductile mode. The ratio of the intergranular area to the transgranular area increased with an increase in cold work level, and the increase in the initial applied stress facilitated the transition in crack morphology to the intergranular mode. In addition, the cold work did not affect the intergranular morphology, whereas the transgranular morphology was significantly affected, and there was typical fan-shaped area on the initial transgranular fracture surfaces of the annealed and mildly cold work specimens. The number of fans increased with the degree of cold work, but the fan pattern became less clear due to extensive dislocation tangling. The results indicate that the divergent direction of fans coincided with the direction of crack propagation[42]. Zheng investigated the stress corrosion cracking behavior of cold-worked (carried out at degrees of 20% and 40%) AISI-type stainless steel in a concentrated lithium salt solution (10 g LiOH and 100 $cm^3$ $H_2O$) with a controlled electrochemical potential. The stress corrosion cracking behavior of the cold-worked specimen was essentially different from that of the solution annealed specimen. The ductile fracturing of cold-worked specimens occurred under open-circuit conditions (-280 $mV_{SCE}$) and at 200 mV. Slight intergranular corrosion was found in the region near the surface of cold-worked specimens when the electrochemical potential was controlled at -120 $mV_{SCE}$. Additionally, stress corrosion cracking was observed when the electrochemical potential was conducted at +100 $mV_{SCE}$, and the intergranular mode in the stress corrosion cracking of the solution annealed specimen transformed into a mixed mode or a dominant transgranular mode with an increase in the degree of cold work to 20% and 40%. The cold work significantly improved the resistance to intergranular stress corrosion cracking compared to that of the solution annealing specimen, and the susceptibility to transgranular stress corrosion of cold-worked specimen increased with an increase in the degree of cold work[43]. Tiedra assessed the effect of cold work on the stress corrosion cracking behaviors of welded and non-welded AISI type stainless steel in a corrosive environment (1 N $H_2SO_4$ and 0.5 N NaCl). The results showed that for the non-welded specimens, the tension strength increased and the failure time (ductility) decreased with increasing the cold work level due to the strain

hardening. However, for the welded specimens, the failure time (ductility) depended on several phenomena (recrystallization, the recrystallized grain growth and thermal transformation of strain-induced martensite) that occurred in the heat affected zone. These phenomena decreased with an increase in the degree of cold work until a level of 20% was reached and then increased. Furthermore, the tension strength did not represent the significant variations in the cold work level, and the failure time was more sensitive to the corrosive environment than was the tension strength for any cold work level. The cold-worked and welded specimens showed a ductile fracture mode in corrosive environment, which was not characteristic of stress corrosion cracking[44].

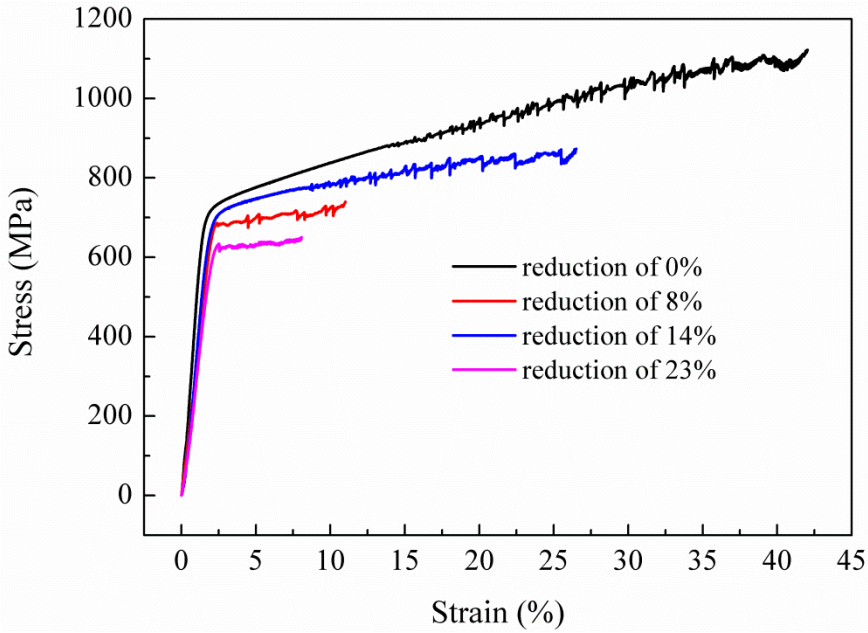


**Figure 3.** Stress-strain curves of SUS 304 stainless steel before and after cold rolling during the slow strain rate test process.

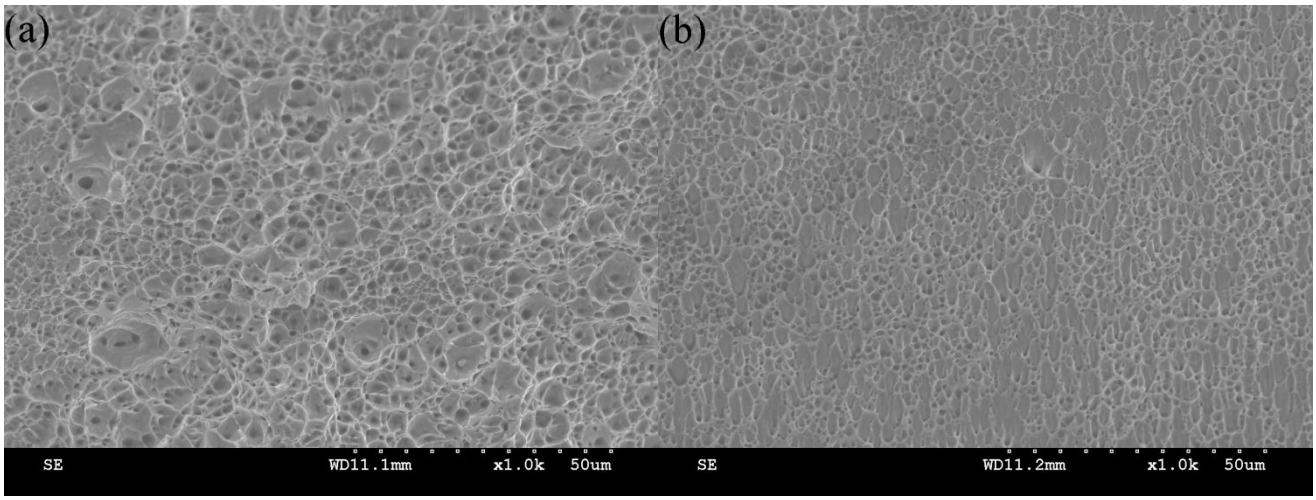

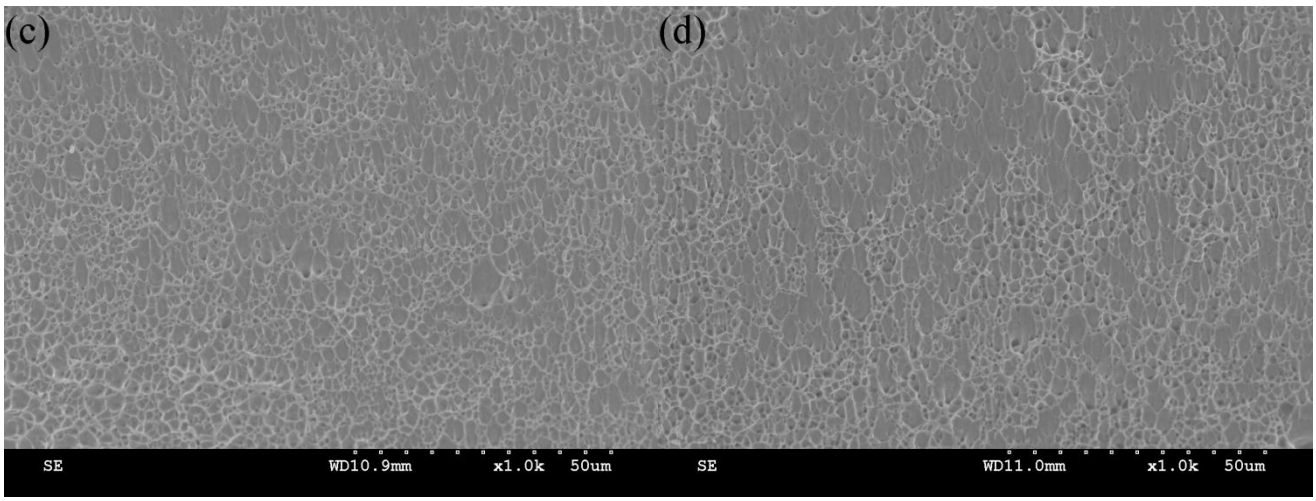


**Figure 4.** Fractographs of SUS 304 stainless steel before and after cold rolling during the slow strain rate test process: (a) specimen before cold rolling; (b) specimen when the degree of rolling reduction was 8%; (c) specimen when the degree of rolling reduction was 14%; and (d) specimen when the degree of rolling reduction was of 23%.

### *3.3 Electrochemical noise analysis with slow strain rate testing*

All of the electrochemical noise data were treated to remove direct the current components before data analysis to obtain accurate analysis results[45,46]. There were several methods for removing the direct current trends such as the moving average removal, and linear and polynomial fitting methods. The polynomial fitting method with 5 orders, considered to be the best way to remove the direct current drift, suppress the low-frequency information and retain the high-frequency information, was employed in this study[47-49]. For instance, Figure 5 displays noise data (obtained from the segment from 0~512 s) of the non-rolled specimen before and after removing the direct current component during the slow strain rate test process. The results indicate that there was an obvious difference between the noise data before and after removal.

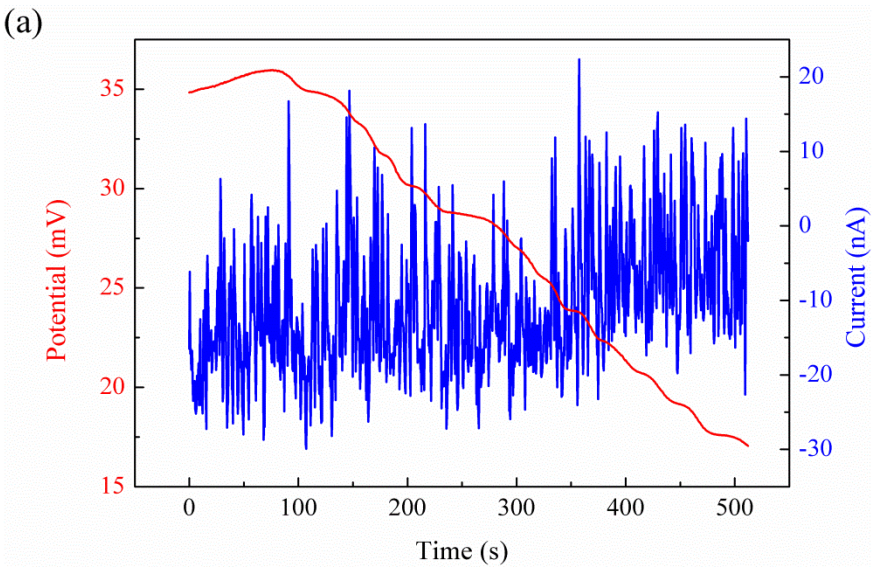

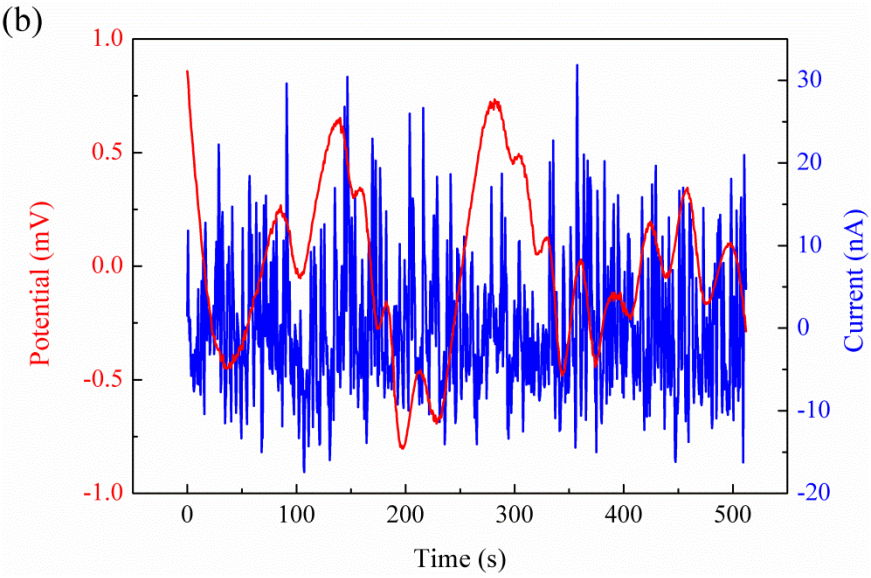


**Figure 5.** Noise data (obtained from the segment from 0~512 s) of the non-rolled specimen before and after removing the direct current component during the slow strain rate test process: (a) before removal; and (b) after removal.

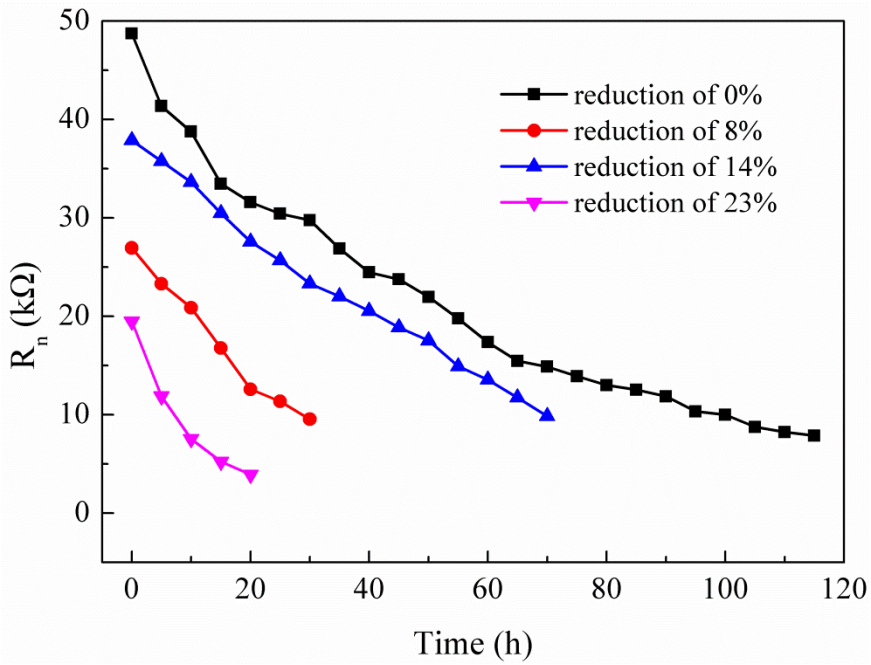


**Figure 6.** Noise resistance $R_n$ of SUS 304 stainless steel before and after cold rolling during the slow strain rate test process.

Figure 6 exhibits the noise resistance $R_n$ of the specimens before and after cold rolling during the slow strain rate test process, which is defined as the ratio of the potential standard deviation to the current standard deviation and is proportional to corrosion resistance[50-53]. As shown, the noise resistance continuously decreased with or without rolling, which indicated that the corrosion resistance of all the specimens presented a continuous deterioration during the slow strain rate test process. The decreasing corrosion resistance could be explained by Gutman′s theory of mechanical-electrochemical

interactions[54], which states that the applied stress could enhance the electrochemical activity of the specimen and a higher applied stress could induce a stronger corrosion tendency; thus, the corrosion resistance was gradually reduced with increasing applied stress during a slow strain rate test process. The noise resistance decreased after cold rolling, which demonstrated that the cold rolling led to a decline in the corrosion resistance of the rolled specimen compared with that of the non-rolled specimen. It should be noted that when the degree of rolling reduction was 14%, the specimen presented the highest corrosion resistance among all the rolled specimens, which agreed with the conclusion obtained from the stress-strain curves in Figure 3.

A frequency domain analysis can estimate the corrosion type through transforming the noise data to a power spectral density (PSD) with a fast Fourier transform (FFT) method[32,55-65].

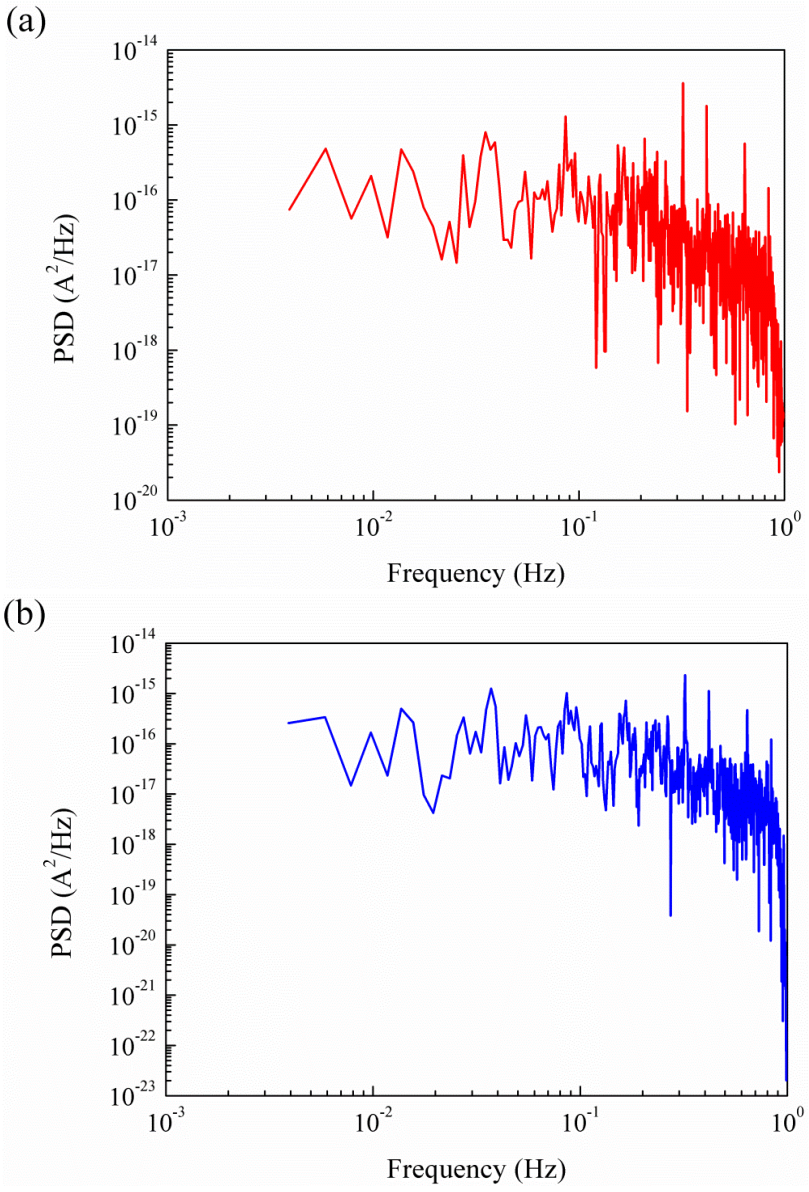


**Figure 7.** PSD (obtained from the segment from 0~512 s) of current noise of the non-rolled specimen before and after smoothing with a Hanning window during the slow strain rate test process: (a) before smoothing; and (b) after smoothing.

For instance, Figure 7 shows the PSD (obtained from the segment from 0~512 s) of current noise of the non-rolled specimen before and after smoothing with a Hanning window during the slow strain rate test process. All of the PSD were smoothed before the frequency domain analysis.

Figure 8 reveals the roll-off slop of the PSD of the current noise of the specimens before and after cold rolling during the slow strain rate test process.

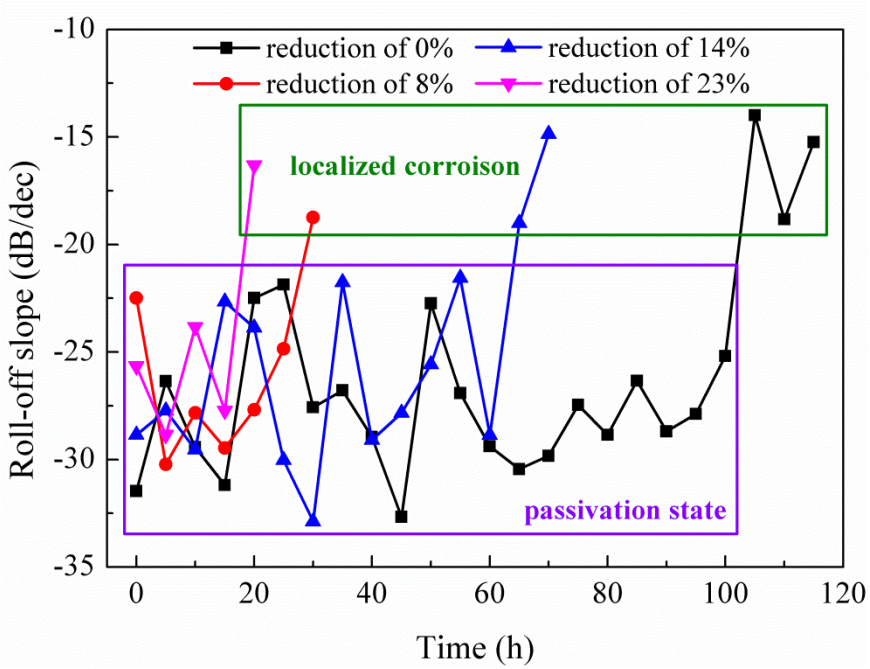


**Figure 8.** Roll-off slop of the PSD of the current noise of SUS 304 stainless steel before and after cold rolling during the slow strain rate test process.

As shown in the figure, for the non-rolled and rolled specimens, when the degree of rolling reduction was 8%, 14% and 23%, the roll-off slop of the PSD was lower than -20 dB/dec in the 0~100 h, 0~25 h, 0~60 h and 0~15 h segments, but higher than -20 dB/dec in the 105~115 h, 30 h, 65~70 h and 20 h segments. Uruchurtu found that the material was in a passivation state when the roll-off slop was lower than -20 dB/dec, and the roll-off slop that was higher than -20 dB/dec represented localized corrosion such as pitting corrosion of the material[66]. Therefore, it could be concluded that there were obvious differences in the occurrence time for the pitting corrosion between the non-rolled and rolled specimens during the slow strain rate test process.

From the above, it was suggested that cold rolling could affect the stress corrosion cracking behavior of SUS 304 stainless steel. The slow strain rate test and electrochemical noise showed that the mechanical properties such as breaking elongation, tension strength and corrosion resistance of the specimen deteriorated after cold rolling. For all of the rolled specimens, when the degree of rolling reduction was 14%, the specimen presented the longest fracture time and highest corrosion resistance during the slow strain rate test process, which means the lowest stress corrosion cracking susceptibility. For the stress corrosion cracking behavior of steel, there is a widely accepted mechanism model that indicates two stages during the slow strain rate test process. In the first stage, the specimen surface can be destroyed and corroded as a result of the synergistic effect of

accumulating tension stress and a corrosive medium during the tension process. The pitting corrosion is considered as the induced source of the crack; thus, the stage is called the crack initiation stage. In the second stage, there is a high level of stress concentration at the crack tip after the crack initiation. The tension stress and a corrosive medium led to dissolution and propagation at the crack tip until the specimen fractures; therefore, the stage is called the crack propagation stage. During the slow strain rate test process, the stress corrosion cracking susceptibility depends on the crack initiation time, which takes up a large part of the total fracture time[67-71]. From the frequency domain analysis results of the current noise of the non-rolled and rolled specimens during the slow strain rate test process, it was quite clear that the non-rolled specimen showed the latest occurrence time of pitting corrosion, which means the longest crack initiation time due to the highest corrosion resistance; therefore, the non-rolled specimen exhibited the lowest susceptibility to stress corrosion cracking. For the rolled specimens during the slow strain rate test process, the pitting corrosion occurred earlier than the non-rolled specimen due to the lower corrosion resistance and was considered to be symbols of the shorter crack initiation time and the higher stress corrosion cracking susceptibility. When the degree of rolling reduction was 14%, the specimen showed the highest corrosion resistance among the rolled specimens; hence, the lowest stress corrosion cracking susceptibility was exhibited because of the late occurrence time of pitting corrosion and the long crack initiation time. In summary, cold rolling played a role as a promoter of SUS 304 stainless steel during the stress corrosion cracking process. However, in this study, by choosing the appropriate degree of rolling reduction (such as 14%), an effective approach to slightly reduce the stress corrosion cracking resistance and significantly enhance the strength at the same time was demonstrated.

## 4. CONCLUSIONS

In this study, the effect of cold rolling on the stress corrosion cracking behavior of SUS 304 stainless steel was investigated by employing electrochemical noise measurements coupled with slow strain rate testing. The results are summarized as follows:

(1) The microstructure of SUS 304 stainless steel transformed from a single austenite phase to a compound of the martensite phase and original austenite phase after cold rolling with various degrees of rolling reduction. An increase in the degree of rolling reduction caused the content of the martensite phase to increase in the SUS 304 stainless steel specimen.

(2) The mechanical properties and stress corrosion cracking susceptibility of SUS 304 stainless steel obviously deteriorated after cold rolling. Compared with the non-rolled specimen, when the degree of rolling reduction was 23%, the breaking elongation and tension strength of the specimen decreased by 81% and 42%, respectively, after cold rolling. Additionally, when the degree of rolling reduction was 14%, the specimen showed the highest mechanical properties and lowest stress corrosion cracking susceptibility among the rolled specimens.

(3) The noise resistance represented a continuous reduction for all the non-rolled and rolled specimens, which implies a decreasing corrosion resistance. The cold rolling process significantly reduced the noise resistance and corrosion resistance, which were highest for the specimen among the

rolled specimens when the degree of rolling reduction was 14%.

(4) The stress corrosion cracking susceptibility depended on the crack initiation time which was determined by occurrence time of pitting corrosion and accounted for a large part of the total fracture time during the slow strain rate test process. Compared with the non-rolled specimen, the pitting corrosion for the rolled specimens occurred much earlier, which means a shorter crack initiation time and a higher stress corrosion cracking susceptibility. Among all the rolled specimens, the specimen exhibited the lowest stress corrosion cracking susceptibility when the degree of rolling reduction was 14% because of the latest occurrence time of pitting corrosion and the longest crack initiation time.

## References

1. M. Mihalikova, M. Hagarova, D. Jakubéczyová, J. Cervová and A. Lišková, *Int. J. Electrochem. Sci.,* 11 (2016) 4206.
2. H.J. Lee and H.W. Lee, *Int. J. Electrochem. Sci.,* 10 (2015) 8028.
3. M.A. Amin, M. Saracoglu, N. El-Bagoury, T. Sharshar, M.M. Ibrahim, J. Wysocka, S. Krakowiak and J. Ryl, *Int. J. Electrochem. Sci.,* 11 (2016) 10029.
4. A. Torres-Islas, A. Molina-Ocampo, R. Reyes-Hernandez, S. Serna, M. Acosta-Flores and J.A. Juarez –Islas, *Int. J. Electrochem. Sci.,* 10 (2015) 10029.
5. A.P.I. Popoola, *Int. J. Electrochem. Sci.,* 9 (2014) 1273.
6. A.H. Ramirez, C.H. Ramirez and I. Costa, *Int. J. Electrochem. Sci.,* 8 (2013) 12801.
7. J. Wang, Y. Liu, Y.F. Qiao, Y.D. Hu, Y.S. Cui and P.D. Han, *Int. J. Electrochem. Sci.,* 12 (2017) 6492.
8. Y.T. Sun, X.Y. Wu, X. Wu, J. Li and Y.M. Jiang, *Int. J. Electrochem. Sci.,* 11 (2016) 9666.
9. L. He, X.Y. Wu, Z.Y. Zhang and J. Li, *Int. J. Electrochem. Sci.,* 11 (2016) 8046.
10. X.Y. Liu, K.D. Xia, J.C. Niu, Z. Xiang, B. Yan and W. Lu, *Int. J. Electrochem. Sci.,* 10 (2015) 9359.
11. B.H. He, J.J. Sun and Q.A. Tu, *Int. J. Electrochem. Sci.,* 10 (2015) 10631.
12. H.W. Wang, C. Yu and S.W. Huang, J. Li, *Int. J. Electrochem. Sci.,* 10 (2015) 5827.
13. H. Liu, *Int. J. Electrochem. Sci.,* 10 (2015) 2130.
14. B. Li, J.H. Wang, X.H. Wang and X. Yue, *Int. J. Electrochem. Sci.,* 11 (2016) 1.
15. W.W. Wu, Y.J. Guo, H.F. Yu, Y.M. Jiang and J. Li, *Int. J. Electrochem. Sci.,* 10 (2015) 10689.
16. C.J. Ortiz-Alonso, J.G. Gonzalez-Rodriguez, J. Uruchurtu-Chavarin and J.G. Chacon-Nava, *Int. J. Electrochem. Sci.,* 10 (2015) 5249.
17. S.S.M. Tavares, J.S. Corte and C.A.B. Menezes, *Eng. Fail. Analy.,* 16 (2009) 552.
18. A.K. Jha, V. Diwakar and K. Sreekumar, *Eng. Fail. Analy.,* 10 (2003) 669.
19. M. Suresh-Kumar, M. Sujata and M.A. Venkataswamy, *Eng. Fail. Analy.,* 15 (2008) 497.
20. R.M. Horn, G.M. Gordon and F.P. Ford, *Nucl. Eng. Design.,* 174 (1997) 313.
21. D.R. Johns and K. Shemwell, *Corros. Sci.,* 39 (1997) 473.
22. H. Okada, Y. Hosoia and S. Abe, *Corrosion,* 27 (1971) 424.
23. S.Szklarska-Snialowska and G. Gragnolino, *Corrosion,* 36 (1980) 653.
24. R. Singh, *J. Mater. Proc. Tech.,* 206 (2008) 286.
25. G. Gragnolino and D.D. Macdonald, *Corros. Sci.,* 38 (1982) 406.
26. H. Li, R.H. Jones and P.J. Hirth, *Warrendale PA:TMS.,* (1996) 219.
27. J.M. Wang and L.F. Zhang, *Anti-Corros. Method. Mater.,* 64 (2017) 252.
28. L. Peguet, B. Malki and B. Baroux, *Corros. Sci.,* 49 (2007) 1933.

29. B. Ravi-Kumar, R. Singh, B. Mahato, P.K. De, N.R. Bandyopadhyay and D.K. Bhattacharya, *Mater. Charact.*, 54 (2005) 141.
30. J.F. Chen and W.F. Bogaerts,*Corros. Sci.*, 52 (1996) 753.
31. D. Gang, W. Weikui, S. Shizhe and J. Shijin, *Anti-Corros. Methods Mater.*, 57 (2010) 126.
32. G. Du, J. Li, W.K. Wang, C. Jiang and S.Z. Song, *Corros. Sci.*, 53 (2011) 2918.
33. M. Mahmoudiniya, S. Kheirandish and M. Asadiasadabad, *Trans. Indian. Inst. Met.*, 70 (2017) 1251.
34. Y.F. Li, F.M. Bu, W.B. Kan and H.L. Pan, *Mater. Manuf. Process.*, 28 (2014) 256.
35. D.N. Wasnik, I.K. Gopalakrishnan, J.V. Yakhmi, V. Kain and I. Samajdar, *ISIJ. International.*, 43 (2003) 1581.
36. N. Mubarok, H.A. Notonegoro, K.A.Z. Thosin and A. Manaf, *AIP Conf. Proc.*, 1746 (2016) 020022-1.
37. S. Palit Sagar, B. Ravi Kumar, G. Dobmann and D.K. Bhattacharya, *NDT&E. Int.*, 38 (2005) 674.
38. J.M. Wang and L.F. Zhang, *Anti-Corros. Methods. Mater.*, 64 (2017) 252.
39. J. Kuniya, I. Masaoka and R. Sasaki, *Corrosion*, 44 (1988) 21.
40. H.S. Khatak, P. Muraleedharan, J.B. Gnanamoorthy, P. Rodriguez and K.A. Padmanabhan, *J. Nucl. Mater.*, 168 (1989) 157.
41. C. Garcia, F. Martin, P. De Tiedra, S. Alonso and M.L. Aparicio, *Corrosion*, 58 (2002) 849.
42. P. Muraleedharan, H.S. Khatak, J.B. Gnanamoorthy and P. Rodriguez, *Metall. Mater. Trans. A.*, 16 (1985) 285.
43. J.H. Zheng and W.F. Bogaerts, *Corrosion*, 49 (1993) 585.
44. P. De Tiedra and Ó. Martín, *Mater. Design.*, 49 (2013) 103.
45. R.A. Cottis, *Corrosion*, 57 (2001) 265.
46. A.M. Hombor, T. Tinga, X. Zhang, E.P.M. Westing, P.J. Oonincx, J.H.W. Wit and J.M.C. Mol, *Electrochim. Acta.*, 70 (2012) 199.
47. Y.J. Tan, S. Bailey, B. Kinsella, Y. Sun and J. Hu, *Corros. Sci.*, 38 (1996) 1681.
48. F. Mansfeld, Z. Sun, C. Hsu and A. Nagiub, *Corros. Sci.*, 43 (2001) 341.
49. U. Bercotti, F. Huet, R. Nogueira and P. Rousseau, *Corrosion*, 58 (2002) 337.
50. D.A. Eden, K. Hladky and D.G. John, *Corrosion*, 86 (1986) 274.
51. F. Mansfeld and H. Xiao, *J. Electrochem. Soc.*, 140 (1993) 2205.
52. G. Gusmano, S. Pacetti, A. Damico, A. Petitti and G. Montesperelli, *Corrosion*, 53 (1997) 860.
53. J.F. Chen and W.F. Bogaerts, *Corros. Sci.*, 37 (1997) 1839.
54. E.M. Gutman, Mechanochemistry and Corrosion Prevention of Metals, *Science Publication*, (1989) Peking, China.
55. R.A. Cottis, A.M. Hombor and J.M.C. Mol, *Electrochim. Acta.*, 202 (2016) 277.
56. B. Ramezanzadeh, S.Y. Arman, M. Mehdipour and B.P. Markhali, *Appl. Surf. Sci.*, 289 (2014) 129.
57. J.L. Luo and L.J. Qiao, *Corrosion*, 55 (1999) 870.
58. T. Anita, M.G. Pujar, H. Shaikh, R.K. Dayal and H.S. Khatak, *Corros. Sci.*, 48 (2006) 2689.
59. M. Leban, V. Dolecek and A. Legat, *Corrosion*, 56 (2000) 921.
60. T. Dorsch, R. Kilian and E. Wendler-Kalsch, *Mater. Corros.*, 49 (1998) 659.
61. J.G. Gonzalez-Rodriguez, M. Casales, V.M. Salinas-Bravo, M.A. Espinosa-Medina and A. Martinez-Villafane, *J. Solid. State. Electr.*, 8 (2004) 290.
62. C.R. Arganis-Juarez, J.M. Malo and J. Uruchurtu, *Nucl. Eng. Des.*, 140 (1993) 2205.
63. Z.M. Shi, G.L. Song, C.N. Cao, H.C. Lin and M. Lu, *Electrochim. Acta.*, 52 (2007) 2123.
64. M. Gomez-Duran and D.D. Macdonald, *Corros. Sci.*, 48 (2006) 1608.
65. J.G. González-Rodriguez, V.M. Salinas-Bravo, E. García-Ochoa and A. Díaz-Sánchez, *Corrosion*, 53 (1997) 693.
66. J.C. Uruchurtu and J.L. Dawson, *Corrosion*, 43 (1987) 19.
67. R.C. Newman, *Corrosion*, 50 (1994) 682.
68. R.C. Newman and C. Healey, *Corros. Sci.*, 49 (2007) 4040.

69. M. Takano and S. Shimodaria, *J. Japan. Inst. Metal.*, 29 (1965) 553.
70. T. Nakayama and M. Takano, *Corros. Sci.*, 37 (1981) 226.
71. T.P. Hoar and J.M. West, *Proc. Roy. Soc.*, 268 (1962) 304.